

Suppression of microRNA-320 Induces Cerebral Protection Against Ischemia/Reperfusion Injury by Targeting HMGB1/NF- κ B Axis

Shaodong LIANG^{1,2}, Wenhui CAO³, Yayan ZHUANG⁴, Deguo ZHANG², Shudi DU², Huaizhang SHI¹

¹Department of Neurosurgery, The First Affiliated Hospital of Harbin Medical University, Harbin, Heilongjiang Province, China, ²Department of Neurosurgery, Hongqi Hospital of Mudanjiang Medical University, Mudanjiang, Heilongjiang Province, China, ³Department of Neurology, Hongqi Hospital of Mudanjiang Medical University, Mudanjiang, Heilongjiang Province, China, ⁴Department of Health Care, Hongqi Hospital of Mudanjiang Medical University, Mudanjiang Heilongjiang Province, China

Received February 14, 2023

Accepted September 15, 2023

Summary

MicroRNAs have been shown to potentially function in cerebral ischemia/reperfusion (IR) injury. This study aimed to examine the expression of microRNA-320 (miR-320) in cerebral IR injury and its involvement in cerebral mitochondrial function, oxidative stress, and inflammatory responses by targeting the HMGB1/NF- κ B axis. Sprague-Dawley rats were subjected to middle cerebral artery occlusion to simulate cerebral IR injury. The cerebral expression of miR-320 was assessed using qRT-PCR. Neurological function, cerebral infarct volume, mitochondrial function, oxidative stress, and inflammatory cytokines were evaluated using relevant methods, including staining, fluorometry, and ELISA. HMGB1 expression was analyzed through Western blotting. The levels of miR-320, HMGB1, neurological deficits, and cerebral infarction were significantly higher after IR induction. Intracerebral overexpression of miR-320 resulted in substantial neurological deficits, increased infarct volume, elevated levels of 8-isoprostane, NF- κ Bp65, TNF- α , IL-1 β , ICAM-1, VCAM-1, and HMGB1 expression. It also promoted the loss of mitochondrial membrane potential and ROS levels while reducing MnSOD and GSH levels. Downregulation of miR-320 and inhibition of HMGB1 activity significantly reversed the outcomes of cerebral IR injury. MiR-320 plays a negative role in regulating cerebral inflammatory/oxidative reactions induced by IR injury by enhancing HMGB1 activity and modulating mitochondrial function.

Key words

Neuroprotection • microRNA • HMGB1 • Inflammation • Oxidative stress

Corresponding author

H. Shi, Department of Neurosurgery, The First Affiliated Hospital of Harbin Medical University, No. 23, Youzheng Street, Nangang District, Harbin, Heilongjiang Province, 150001, China. E-mail: shihuaizhang01@sina.com

Introduction

Stroke is a leading cause of disability and death worldwide. Cerebral ischemia is the most common type of stroke, accounting for approximately 80 % of all cases [1]. Restoring blood flow, known as reperfusion, is a desirable therapeutic approach for acute stroke management [2]. However, spontaneous reperfusion damage occurs in about 50-70 % of individuals with ischemic stroke, significantly exacerbating the functional outcomes of the stroke. Despite advancements in therapeutic treatments such as thrombolytic or endovascular therapy aimed at limiting the progression of reperfusion damage, mortality rates remain high, making stroke treatment a complex clinical challenge [1,2]. This is primarily due to the involvement of various pathophysiological processes, and understanding these critical mechanisms could contribute to the development

of novel and more effective therapeutic options.

Experiments have shown that oxidative stress, inflammatory responses, leukocyte infiltration, and mitochondrial-driven pathways are all essential factors in cerebral ischemia-reperfusion (IR) injury [2,3]. When the production of reactive oxygen species (ROS), including peroxide and free radicals such as superoxide anions, surpasses the antioxidant capacity during an IR insult, oxidative stress develops. During the reperfusion phase, mitochondria emerge as a primary source of ROS generation [4]. IR conditions have been demonstrated to cause post-translational alterations in oxidative phosphorylation proteins, increasing mitochondrial membrane potential and resulting in ROS overproduction [4]. Additionally, the pathophysiology of cerebral IR damage is heavily influenced by inflammation, with leukocyte infiltration being a significant initiating factor [5,6]. Activated leukocytes adhere to endothelial cells through chemotactic signals, leading to the synthesis of matrix metalloproteinase and neutrophil-derived oxidants, ultimately disrupting the blood-brain barrier. Subsequently, leukocytes traverse capillaries and enter brain tissues, activating cytokines that trigger inflammation and contribute to the deterioration of the penumbra region [3].

High mobility group box-1 (HMGB1) is a protein expressed in most tissues and released in significant amounts into the extracellular fluid following cerebral ischemia and related injuries, exacerbating oxidative and inflammatory processes after IR damage [7]. Excess HMGB1 has an affinity for binding pro-inflammatory molecules such as IL-1 β , IL-6, and adhesive proteins. HMGB1^{-/-} mouse cells, deficient in type I interferon and inflammatory cytokines, show hindered activation of the nuclear factor (NF)- κ B pathway. HMGB1 triggers the toll-like receptor (TLR)-4 complex, leading to NF- κ B-dependent production of inflammatory transcripts [8,9]. Consequently, inhibiting HMGB1 activity can mitigate inflammation and subsequent brain damage during ischemia and reperfusion.

MicroRNAs (miRs) influence the expression of target genes, thereby modulating a range of biological processes [10]. Due to their critical roles in various disorders, including brain complications, miRs are recognized for their involvement in regulating key signaling factors in cerebral IR damage [11]. Prior research has identified distinct expression patterns of miR-320 in various tissues, such as the heart, spinal cord,

and brain, following ischemic injuries [12-15]. These studies have reported both increased and decreased expression of miR-320. Intriguingly, elevated miR-320 expression during IR conditions has been observed to exacerbate the injury. For instance, in mouse cardiomyocytes, heightened miR-320 expression promoted apoptotic death and mitochondrial dysfunction by targeting the AKIP1 protein [13]. Conversely, another study found decreased miR-320 expression in murine cardiomyocytes subjected to IR, and its overexpression increased heart sensitivity to IR injury by targeting heat-shock protein-20 [16]. MiR-320 also accelerated brain parenchymal injury by modulating insulin-like growth factor-1 in mice [14]. Furthermore, miR-320 appears to regulate metabolic abnormalities caused by oxidative stress [17]. Reports suggest that miR-320 might target HMGB1 [11,18], and the levels of miR-320 expression could influence the outcomes of cerebral IR damage by affecting the HMGB1 pathway. Therefore, it is hypothesized that the miR-320/HMGB1/NF- κ B signaling pathway could be a valuable target for managing cerebral IR. However, there are conflicting findings on the expression of miR-320 in the brain, and it remains unclear whether and how cerebral IR damage is affected by the miR-320 and HMGB1 signaling pathway. Consequently, the aim of this study was to investigate the involvement of miR-320 in regulating cerebral IR injury and modulating mitochondrial function, oxidative stress, and inflammatory responses in the brain by targeting the HMGB1/NF- κ B axis.

Materials and Methods

Animals

Seventy two Sprague-Dawley rats weighing between 250 and 300 g were provided from the Laboratory Animal Centre and housed in a 12 h cycle of lightness/darkness at a normal housing temperature of 24 °C and humidity of 55 %. Each cage held five rats, and they were given free access to food and water. All animal experiments and handling techniques were carried out with the permission of the University Animal Ethics Committee.

Cerebral IR injury modeling

Based on previous research, the middle cerebral artery occlusion (MCAO) model was employed to simulate cerebral IR injury. The animals were anesthetized with an intraperitoneal injection of sodium

pentobarbital (40 mg/kg; Sigma-Aldrich; Germany). Following exposure of the right carotid arteries, a monofilament thread with a diameter of 0.24 mm was carefully inserted into the internal carotid artery and gently advanced for 18–20 mm from the carotid bifurcation to occlude the origin of the middle cerebral artery, inducing ischemia. All these procedures were completed within approximately 15 min. The thread was left in place for a duration of two hours before being removed to initiate reperfusion. Throughout the experiment, a heating pad was used to maintain the rats' rectal temperature at 37.5 °C, and the administration of anesthetic was repeated every 50–60 min based on the specific requirements of each animal. Once reperfusion was established, the incision site (muscle and skin) was sutured, allowing the rats to undergo a recovery period. After 24 h of reperfusion, the rats were subjected to behavioral tests and then they were re-anesthetized with sodium pentobarbital (40 mg/kg) and sacrificed for tissue sampling. The rats in the sham group underwent an identical procedure, except for the arterial occlusion. Rats exhibiting severe bleeding, hemorrhaging, or premature death were excluded from the study.

Animal grouping and treatments

Rats were divided into the following six groups at random (n=12): 1) Sham; 2) IR; 3) IR + miR-320 mimic (miR-320); 4) IR + miR control (C-miR); 5) IR + antagomiR-320 (antimiR); and 6) IR + antiHMGB1 (antiHMGB). For miR mimic and control treatments, the rats were firstly anesthetized with sodium pentobarbital (40 mg/kg) and located in a stereotaxic device (Life Science, Shenzhen, China). The stereotaxic coordinates

were set at axes of 0.3 mm anteroposterior, 1.0 mm mediolateral, and 2.5 mm depth. Then, 100 μM/3 μl miR-320 mimic or miR control (supplied by GenePharma, Shanghai, China) were diluted in Entranster™ transfection reagent (Engreen, Beijing, China) and injected into ipsilateral cerebral ventricle 2 h before MCAO using a Hamilton microsyringe. The syringe was left in place for 20 min to allow the solution to diffuse locally [14]. AntagimiR-320 (50 μg) and HMGB1 antagonist (HMGB1 a box) (50 μg/kg; HM-012, Milano, Italy) were injected intravenously *via* tail vein in 0.3 ml PBS to rats, 30 min before and 3 h after the onset of occlusion [19]. Untreated IR animals received intravenously the same volume of PBS at the appropriate time point. Additionally, a separate group of animals in the IR group underwent stereotaxic surgery and received a vehicle without any additional interventions, serving as the stereotaxic control. As the results of this group showed no significant differences compared to the C-miR group, their data was excluded from the analysis to simplify data presentation and enable better comparisons between groups in figures. After recovery from MCAO surgery and after 24 h of reperfusion, rats were assessed for neurologic impairments, and then their brains were extracted for analysis. Once the brain has been removed under anesthesia with sodium pentobarbital (40 mg/kg), the carcasses of rats were disposed of using an aseptic approach. Six rats were considered for infarct volumes measurements and six rats for other cellular and molecular evaluations. The timeline sequence of interventions in rats for the current study is depicted in Fig 1.

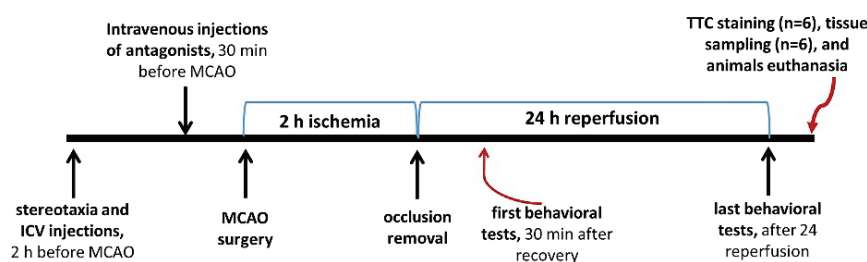


Fig. 1. Schematic diagram showing the timeline for interventions and procedure in the current study. IR: ischemia-reperfusion; miR: microRNA; C-miR: microRNA control; antimiR: microRNA inhibitor; antiHMGB: HMGB1 antagonist. TTC: 2,3,5-triphenyltetrazolium chloride. i.v.: intravenously; ICV: intracerebroventricular; MCAO: middle cerebral artery occlusion.

Animal Groups	Description
Sham	Surgical procedures, except for arterial occlusion
IR	Induction of ischemia-reperfusion, 0.3 ml PBS, i.v. 30 min prior to MCAO
IR + miR320 (miR320)	Induction of ischemia-reperfusion, 100 μM/3 μl miR-320 mimic, ICV, 2 h prior to MCAO
miR control (C-miR)	Induction of ischemia-reperfusion, 100 μM/3 μl miR control, ICV, 2 h prior to MCAO
IR + antagomiR-320 (antimiR)	Induction of ischemia-reperfusion, AntagimiR-320 (50 μg/rat), i.v., 30 min prior to MCAO
IR + antiHMGB1 (antiHMGB)	Induction of ischemia-reperfusion, AntagimiR-320 (50 μg/kg), i.v., 30 min prior to MCAO

We chose two administrative routes of drugs due to some factors including the injection frequency, pharmacokinetics, previous literature evidence, and technical feasibility. Administration of miR-320 mimic and miR control directly into the cerebral ventricle allows for targeted delivery to the brain tissue. Considering the ease of crossing the blood-brain barrier and previous studies demonstrating convenient administration *via* the intravenous route, the antagonists were injected twice *via* intravenous injection [20,21]. This choice was made to facilitate the intervention and minimize brain manipulation in the animals.

Neurological deficits rating

Neurological deficits rating was performed 30 min after recovery from MCAO surgery, to confirm the successful occlusion, and at the end of reperfusion time (24 h after MCAO surgery). Animals' recovery was carefully monitored to ensure that they were in an appropriate neurological and consciousness state for evaluation. More serious cerebral damage is indicated by a higher rating in this system. Neurological findings were graded using a 5-point scale, with 0 representing no neurological impairment symptoms, 1 representing failing to fully extend the left paw, 2 representing rotating to left, 3 representing falling to the left, and 4 representing no spontaneous walking and very low levels of consciousness [22].

Corner test and adhesive removal test

The sensorimotor function and postural asymmetries of rats was tested using the Corner test and adhesive removal test, at baseline (pre-stroke) and 24 h post-stroke, as described previously [22]. In corner test, the rats were permitted to move through a tunnel and then into a corner with a 60-degree angle. To exit this corner, the rats could turn either to left or right. The test was repeated for 10 to 15 trials, ensuring at least a 30-second intervals. The counts of left and right turns from 10 successful trials for each rat were documented and reported. Then, the Corner test score was calculated as: $[(\text{right turns}) / (\text{right turns} + \text{left turns})] \times 100$. In adhesive removal test, two adhesive tapes of equal size (3×4 mm) were gently attached to the hairless area of both forepaws of rats as tactile stimuli. The study measures sensorimotor performance by recording the time it takes for the rat to make initial contact with each paw and the subsequent time it takes to remove the adhesive tape from each side (time-to-remove). This

allows for the differentiation of sensory and motor deficits. Animals with unilateral brain damage typically display a preference for faster removal from the unaffected ipsilateral limb. The rats experienced a four-day training before MCAO surgery to ensure accurate assessment. A researcher blinded to animal grouping performed both tests.

Measurement of cerebral infarction

Six rat's brains from each group were instantly removed under anesthesia, immediately frozen at -20 °C and placed in a brain matrix. Then, 2-mm thick coronal slices were done on samples using a sharp blade. The slices underwent staining with 2,3,5-triphenyl tetrazolium chloride (2 %) (Sigma-Aldrich; Germany) for 25 min at 37 °C, and then left in 4 % paraformaldehyde overnight. Then, digital images were taken from the stained slices and the penumbra and infarcted areas were identified with the software ImageJ (NIH, Bethesda; USA). Brain infarct volumes were calculated as infarcted area percentages and normalized to the animal's brain volume.

Measurement of mitochondrial activity and intracellular oxidative stress

First, the mitochondrial content was obtained from the brain samples from the ipsilateral cortex's peripheral penumbra. For this purpose, the samples were homogenized in a mitochondrial isolation buffer having a protease inhibitor (Sigma Aldrich, USA) and centrifuged at 10000 rpm for ten minutes. To acquire the mitochondrial fraction, the resultant pellets were re-centrifuged at 21000 rpm. Using a BCA kit (Beyotime, China), the sample's total protein was measured. For determination of the levels of mitochondrial ROS, 2 μM dichlorodihydrofluorescein diacetate dye (Sigma Aldrich, USA) was mixed with supernatant and held at 37 °C for 30 min. Following that, the solution was excited at 480 nm and its emission absorbance was read at 530 nm, fluorometrically, the excitation and emission were measured. To estimate the changes of mitochondrial membrane potential, 2 μl cationic carbocyanine JC-1 dye (Sigma Aldrich, USA) was mixed with 100 μl of mitochondrial supernatant and held in the dark place for 30 min at 37 °C. The extent of mitochondrial membrane depolarization was calculated fluorometrically using the red to green ratio of fluorescence intensities of JC-1 in each sample. The mitochondrial ROS and membrane potential values were reported after being normalized to

the protein concentrations of samples. Furthermore, the supernatants were used to evaluate the contents of 8-isoprotane, a lipid peroxidation marker, mitochondrial manganese-superoxide dismutase (Mn-SOD), and glutathione (GSH) using ELISA kits, based on the manufacturer instructions (Sigma Aldrich, USA). The absorbance value of the samples was read at 450 nm, spectrophotometrically, and normalized to total protein content.

Measurement of adhesive molecules and cytokines

At the end of reperfusion, the brain sample was obtained from ipsilateral cortex of animals and then homogenized in a lysing buffer (Beyotime, China), followed by centrifugation at 10000 rpm. Thereafter, the supernatant was collected for the measurement of the content of proinflammatory cytokines NF- κ Bp65, TNF- α , and IL-1 β , along with the content of intercellular adhesion molecule-1 (ICAM-1) and vascular cell adhesion molecule-1 (VCAM-1). The cytokines and adhesion molecules were assessed using rat-specific commercially available kits (MyBioSource, USA) through ELISA method, based on the provided instructions. The provided micro ELISA plate was coated with antibodies specific to the mediators of interest. Standards or samples were added to the plate wells and incubated with the specific antibody, followed by the addition of the Avidin-HRP conjugate. After washing away unbound components, a substrate solution was added, and the reaction was then stopped with a stop solution. The optical densities were measured at 450 nm, and these values were utilized to calculate the concentrations of the mediators using the corresponding standard curve.

Real time PCR

RNeasy Mini Kit (Qiagen, USA) was employed to extract total RNA from brain samples. Using the DNA-free DNA Removal Kit (ThermoFisher Scientific, USA), contamination was eliminated. Then, a High Capacity cDNA Reverse Transcription Kit (ThermoFisher Scientific, USA) was used to reverse transcript RNA and cDNA synthesis. The forward and reverse primers for miR-320 were provided and utilized in real time PCR. Each PCR sample was run in triplicate. A PowerUP SYBR Green Master Mix (ThermoFisher Scientific, USA) was used to measure relative gene expression levels in accordance with the manufacturer's instructions under the thermal cycler conditions of: 2-min 50 °C,

2-min 95 °C, 40 cycles of 1-s 95 °C and 30-s 60 °C, and 4 °C hold. MiR-320 expression was normalized to the expression of internal control U6, and the relative expression was calculated.

Immunoblotting

In brain samples, the expression of HMGB1 and GAPDH proteins was determined using the Western blot technique. Each sample's proteins (about 20 μ g) were separated by sodium dodecyl sulfate-polyacrylamide gel electrophoresis and transferred to a polyvinylidene difluoride (PVDF) membrane (ThermoFisher Scientific, USA). The membranes were then blocked for an hour in 5 % skim milk with 0.1 % Tween-20. The target protein primary antibodies (1:1500, Novus Biologicals, USA) were then applied to the blocked membranes at 4 °C overnight, followed by three washes with Tris buffer saline (TBS). Then, the horseradish peroxidase (HRP)-conjugated secondary antibody (1:2500, Cell Signaling, USA) was applied for an hour to develop specific binding. The membrane was then rinsed in TBS and incubated in the darkroom with the enhanced chemiluminescence reagents before being subjected to the X-ray film. The protein bands and their corresponding intensities were observed. Image J software (NIH, USA) was used to detect the protein bands of HMGB1 which their intensities were then normalized to GAPDH intensity of the samples.

Statistical analyses

Experimental data were reported as means and standard deviation (SD). Normally distributed data between groups were analyzed using one-way ANOVA with Tukey *post hoc* test. $p < 0.05$ was considered as statistically significant.

Results

Overexpression of miR-320 exacerbated cerebral IR injury and increased IR-induced sensorimotor impairment and neurological deficit

Behavioral function was evaluated by the neurological deficits rating, corner test, and adhesive removal test, and cerebral infarction was quantified by TTC staining following MCAO-induced cerebral IR injury. When compared to the Sham group, the rats treated with MCAO exhibited larger infarct volumes and more significant neurological impairment, as indicated by higher scores on neurological deficits, reduced corner test

scores, and increased delays in removing adhesive tape from the affected limb ($p < 0.001$), demonstrating that cerebral IR injury had been successfully induced (Fig. 2). After 24 h of reperfusion, the rats treated with miR-320 exhibited significantly larger infarct sizes and more pronounced sensorimotor and neurological deficits compared to the IR group ($p < 0.05$), while the effect of control mimic was not statistically significant (Fig. 2). Inhibition of miR-320 activity through administration of anti-miR-320 significantly abolished the detrimental effect of miR-320 on infarct volumes and neurological findings ($p < 0.001$), and reduced the outcomes of cerebral IR injury as compared with IR rats ($p < 0.01$). In addition, blockade of HMGB1 activity also had significant neuroprotective effects and considerably reduced the effects of miR-320 on cerebral infarct volumes and behavioral activity ($p < 0.01$) (Fig. 2).

Overexpression of miR-320 exacerbated mitochondrial activity during cerebral IR injury

To estimate mitochondrial activity, alterations of mitochondrial membrane potential and levels of ROS were measured. In comparison to the Sham group, cerebral IR damage depolarized mitochondrial membrane potential (reduced potential) (Fig. 3A and B) and dramatically increased the levels of mitochondrial ROS ($p < 0.001$) (Fig. 3C). Although the miR-320 mimic treatment had no statistically significant effect on the mitochondrial parameters, administration of anti-miR-320 significantly reduced IR-induced reduction of membrane potential and production of mitochondrial ROS levels ($p < 0.01$). Interestingly, inhibition of HMGB1 IR injury considerably reversed IR-triggered alterations in mitochondrial function ($p < 0.05$).

Overexpression of miR-320 exacerbated oxidative stress during cerebral IR injury

The cerebral levels of 8-isoprostane, as a main peroxidation marker, reduced and the levels of MnSOD and GSH, as the endogenously active enzymatic antioxidants, significantly increased in IR group comparing to Sham rats ($p < 0.001$) (Fig. 4A-C). Overexpression of miR-320 a significantly elevated IR-induced elevation of 8-isoprostane and further reduced the levels of GSH ($p < 0.05$). However, administration of anti-miR-320 or anti-HMGB1 significantly hindered the effect of IR injury on the cerebral levels of 8-isoprostane, MnSOD and GSH, as compared with the IR or miR-320 groups ($p < 0.05$).

Overexpression of miR-320 exacerbated inflammatory reactions during cerebral IR injury

ICAM-1 and VCAM-1 expression as well as the production of proinflammatory mediators including NF- κ Bp65, TNF- α , and IL-1 β increased considerably in rats after in-vivo cerebral IR injury ($p < 0.001$) (Fig. 5A-E). Administration of miR-320 mimic was capable to further increase IR-induced production of adhesive molecules and proinflammatory cytokines ($p < 0.05$, and $p < 0.01$). However, the expression levels of ICAM-1 and VCAM-1, along with the levels of NF- κ Bp65, TNF- α , and IL-1 β were significantly downregulated after administration of anti-miR-320 and antagonist of HMGB1, as compared to those of IR or miR-320 groups ($p < 0.001$). Blocking of HMGB1 activity had considerably more protective effects against IR-induced inflammatory reactions than anti-miR-320 administration ($p < 0.05$) (Fig. 5).

Overexpression of miR-320 upregulated the expression of HMGB1 during cerebral IR injury

As seen in Figure 6, rats with cerebral IR injury had considerably higher levels of HMGB1 protein expression than those in the control group ($p < 0.01$). Overexpression of miR-320 significantly increased the expression of this protein following cerebral IR injury as compared to the IR group ($p < 0.001$). Anti-miR-320 and anti-HMGB1 treatments resulted in a considerable downregulation of HMGB1 in the rat brain tissue when compared to the IR and miR-320 groups ($p < 0.001$).

Expression profile of miR-320 in different experimental groups during cerebral IR injury

Following the induction of cerebral IR injury, the expression of miR-320 significantly upregulated as compared to the Sham group ($p < 0.01$) (Fig. 7). Obviously, the expression of miR-320 was the greatest in group receiving miR-320 mimic ($p < 0.001$ vs. IR group). However, administration of anti-miR significantly suppressed the expression of miR-320 ($p < 0.01$). At the last but not the least, blocking of HMGB1 activity had no effect on the expression of miR-320 when compared to the IR group (Fig. 7).

Discussion

In this study, it was revealed that miR-320 exacerbates cerebral injury in rats subjected to IR by increasing oxidative stress, inflammatory responses, and mitochondrial dysfunction. Administration of anti-miR-320

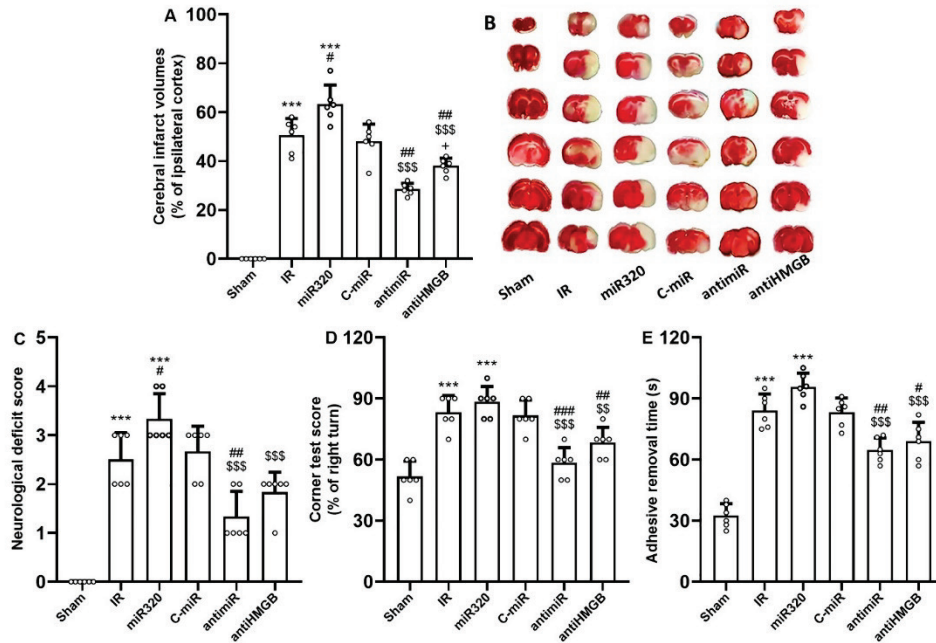


Fig. 2. MiR-320 exacerbated cerebral IR injury and its inhibition had neuroprotective effect. (A) cerebral infarct volumes, (B) TTC staining of brain slices, (C) neurological deficit score, (D) corner test score, and (E) adhesive removal time. Neurological deficit scoring assesses the movement impairments. Similarly, the corner test score and adhesive removal time evaluate the sensorimotor function and postural asymmetries. Induction of IR injury and overexpression of miR-320 in IR setting exacerbated behavioral tests scores and infarct volumes, while both anti-miR and antiHMGB induced neuroprotection after 24 h reperfusion. The data was provided as mean ± SD. N=6. *** p<0.001 vs. Sham group, # p<0.05, and ## p<0.01 vs. IR group, \$\$\$ p<0.001 vs. miR-320, + p<0.05 vs. anti-miR group. IR: ischemia-reperfusion; miR: microRNA; C-miR: microRNA control; anti-miR: microRNA inhibitor; antiHMGB: HMGB1 antagonist.

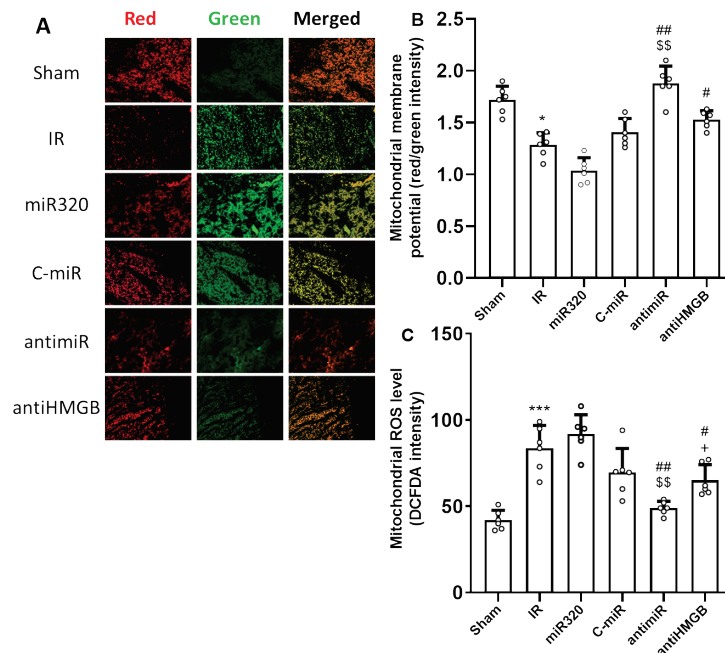


Fig. 3. MiR-320 impaired cerebral IR injury-induced mitochondrial function and its inhibition had mitoprotective effect. (A) JC-1 red/green fluorescence staining for measurement of mitochondrial membrane potential, (B) the results of JC-1 red/green fluorescence intensity indicating mitochondrial membrane potential level, and (C) the results of DCFDA fluorescence intensity indicating mitochondrial ROS level. In measurement of mitochondrial membrane potential (A), the red signal corresponds to aggregated JC-1 dye, which occurs in active mitochondria with higher membrane potential, while the green signal represents the monomeric form of JC-1 dye, which occurs in dysfunctional or depolarized mitochondria with lower membrane potential. Induction of IR injury reduced mitochondrial function, while both anti-miR and antiHMGB improved mitochondrial function. The data was provided as mean ± SD. N=6. * p<0.05, and *** p<0.001 vs. Sham group, # p<0.05, and ## p<0.01 vs. IR group, \$\$\$ p<0.001 vs. miR-320, + p<0.05 vs. anti-miR group. IR: ischemia-reperfusion; miR: microRNA; C-miR: microRNA control; anti-miR: microRNA inhibitor; antiHMGB: HMGB1 antagonist.

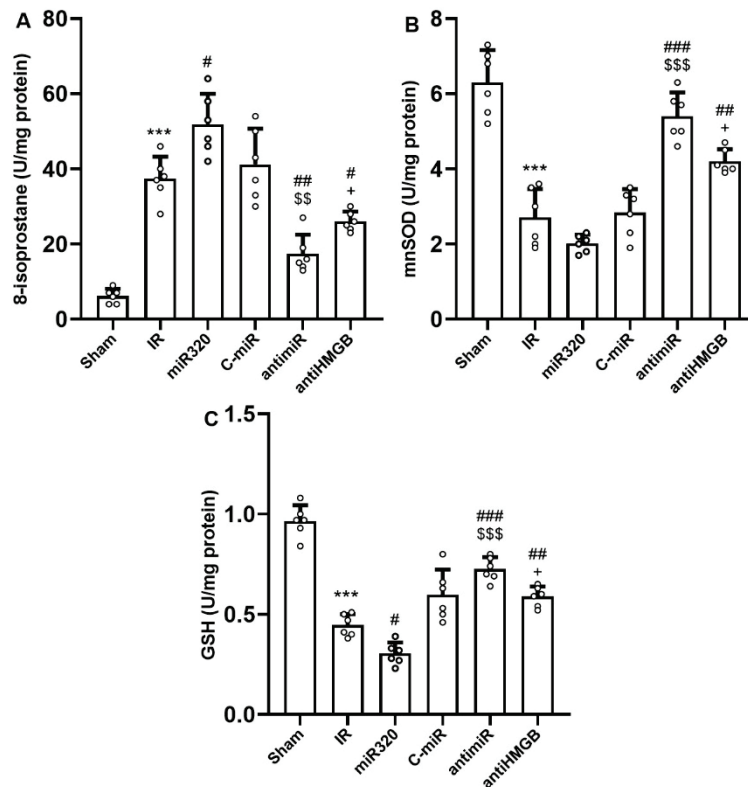


Fig. 4. MiR-320 worsened cerebral IR injury-induced oxidative stress and its inhibition had antioxidative effect. **(A)** 8-isoprostane levels, **(B)** MnSOD levels, and **(C)** GSH glutathione levels. 8-isoprostane is a main indicator of oxidative stress, while MnSOD and GSH are two main endogenous antioxidants. Induction of IR injury and overexpression of miR-320 in IR setting triggered oxidative stress, while both anti-miR and antiHMGB had anti-oxidative effects. The data was provided as mean \pm SD. $N=6$. ** $p<0.01$, and *** $p<0.001$ vs. Sham group, # $p<0.05$, ## $p<0.01$, and ### $p<0.001$ vs. IR group, \$ $p<0.01$, and \$\$\$ $p<0.001$ vs. miR-320, + $p<0.05$ vs. anti-miR group. IR: ischemia-reperfusion; miR: microRNA; C-miR: microRNA control; anti-miR: microRNA inhibitor; antiHMGB: HMGB1 antagonist.

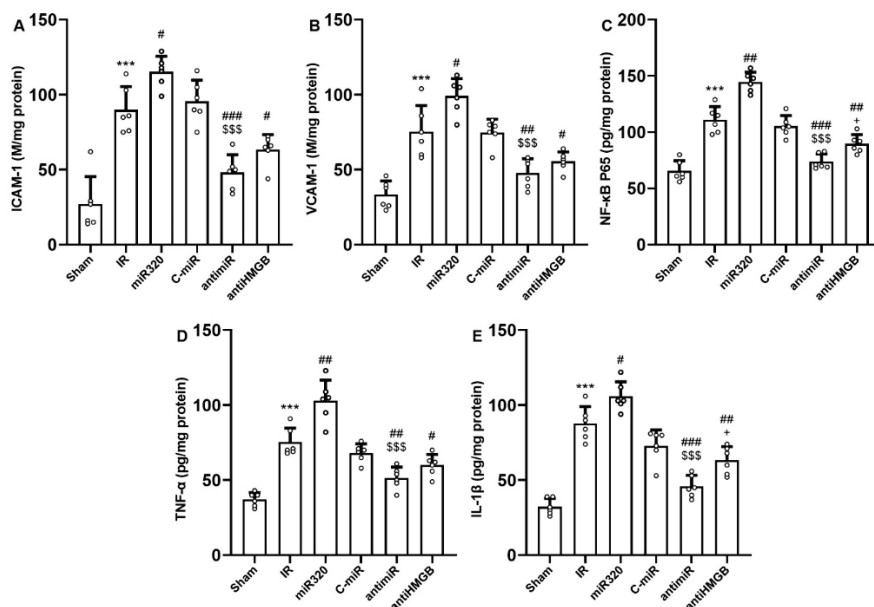


Fig. 5. MiR-320 intensified cerebral IR injury-induced inflammatory responses and its inhibition had anti-inflammatory effect. **(A)** ICAM-1, **(B)** VCAM-1, **(C)** NF- κ B p65, **(D)** TNF- α , and **(E)** IL-1 β . ICAM-1 or intercellular adhesion molecule-1, and VCAM-1 or vascular cell adhesion molecule-1 are adhesive proteins essential for orchestrating inflammation by interacting with vascular endothelial cells. NF- κ B, TNF- α , and IL-1 β are key molecular components in cytokine-driven inflammatory responses. Induction of IR injury and overexpression of miR-320 in IR setting triggered inflammatory responses, while both anti-miR and antiHMGB had anti-inflammatory effects. The data was provided as mean \pm SD. $N=6$. ** $p<0.01$, and *** $p<0.001$ vs. Sham group, # $p<0.05$, ## $p<0.01$, and ### $p<0.001$ vs. IR group, \$ $p<0.01$, and \$\$\$ $p<0.001$ vs. miR-320, + $p<0.05$ vs. anti-miR group. IR: ischemia-reperfusion; miR: microRNA; C-miR: microRNA control; anti-miR: microRNA inhibitor; antiHMGB: HMGB1 antagonist.

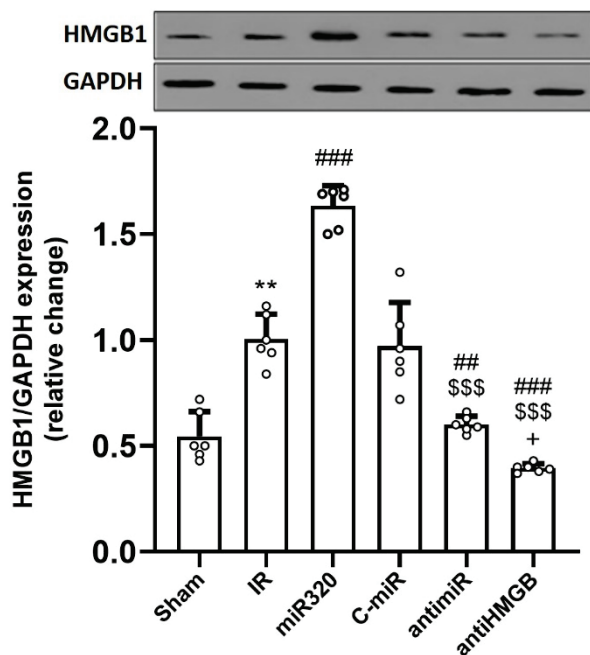


Fig. 6. MiR-320 increased protein expression of HMGB1 following cerebral IR injury and its inhibition had opposite effect. HMGB1 or high mobility group box 1, is a protein that plays a significant role in various biological processes, including inflammation, immunity, and DNA organization. Induction of IR injury and overexpression of miR-320 in IR setting upregulated the expression of HMGB1 protein, while both anti-miR and antiHMGB suppressed its expression. The data was provided as mean \pm SD. N=6. ** p <0.01 vs. Sham group, ## p <0.01, and ### p <0.001 vs. IR group, \$\$\$ p <0.001 vs. miR-320, + p <0.05 vs. anti-miR group. IR: ischemia-reperfusion; miR: microRNA; C-miR: microRNA control; anti-miR: microRNA inhibitor; antiHMGB: HMGB1 antagonist.

or anti-HMGB1 improved behavioral tests, reduced infarct volumes, and led to favorable changes in biochemical parameters in the IR setting. The overexpression of miR-320 upregulated cerebral HMGB1 expression and exacerbated IR injury. These results indicate that miR-320's negative impact on neuroprotection during IR injury is partly mediated by increased HMGB1 activity.

The pro-apoptotic and pro-oxidative actions of miR-320 have been observed in other tissues, such as the heart and osteoblasts [13,23]. Our findings further support the notion that miR-320 possesses pro-oxidative and pro-inflammatory properties in cerebral tissue under IR conditions. Overexpression of miR-320 in the brains of rats with IR led to an increase in 8-isoprostane, a lipid peroxidation index, and mitochondrial ROS levels in cerebral tissue, while endogenous antioxidants MnSOD and GSH were reduced. These findings demonstrate the accumulation of IR-induced oxidative damage in rats. Excessive inflammatory responses and oxidative stress exacerbate tissue damage during cerebral IR injury [3].

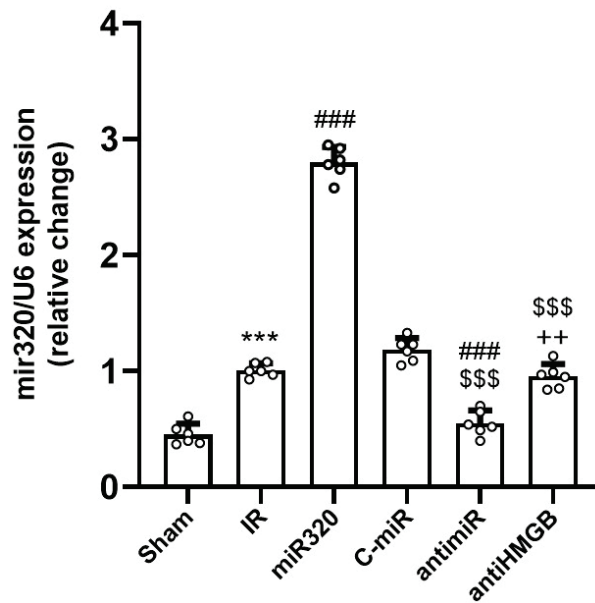


Fig. 7. The expression of miR-320 in different groups following cerebral IR injury. The level of miR-320 expression was quantified relative to the expression of U6 as the internal control to assess its alterations under different conditions. IR induction increased miR-320 expression, while administration of anti-miR suppressed its expression. Administration of antiHMGB had no effect on IR-induced miR-320 expression. The data was provided as mean \pm SD. N=6. *** p <0.001 vs. Sham group, ### p <0.001 vs. IR group, \$\$\$ p <0.001 vs. miR-320, ++ p <0.01 vs. anti-miR group. IR: ischemia-reperfusion; miR: microRNA; C-miR: microRNA control; anti-miR: microRNA inhibitor; antiHMGB: HMGB1 antagonist.

Circulating inflammatory cells are recruited to injured cerebral tissue, leading to the release of endothelial-dependent adhesive proteins and pro-inflammatory cytokines [24]. Excessive ROS generated during reperfusion can also trigger an inflammatory response, further worsening IR injury [3,4]. Accordingly, we found that the administration of anti-miR-320 reduced the expression of ICAM-1, VCAM-1, TNF- α , IL-1 β , and NF- κ Bp65, all of which were elevated in the cerebral tissue of rats after IR damage. NF- κ B signaling, a transcription factor regulating inflammation, oxidative stress, and apoptosis, is activated during the early stages of neuropathy induction, leading to increased cytokine release, inflammatory reactions, and heightened oxidative stress sensitivity in neural cells under IR conditions in rats [25].

NF- κ B activation in the brain involves two main pathways: the canonical and noncanonical pathways. The canonical pathway is initiated by signals like cytokines, ROS, and neurotransmitters, sensed by receptors such as TLRs and IL-1 β receptors [25]. This prompts NF- κ B translocation to the nucleus, triggering gene transcription.

The noncanonical pathway responds to TNF family ligands, processing the NF- κ B precursors [25]. Besides its pro-inflammatory function, NF- κ B has been proposed to have some protective effects in cerebral ischemia. For instance, this transcription factor has the potential to exhibit anti-apoptotic properties by inhibiting caspase 8 activity or promoting the expression of Bcl2 family proteins [26]. It displays diverse effects in different neural cell types, such as neurons and glial cells, especially under various pathological conditions. The interaction between the canonical and noncanonical pathways of NF- κ B activation appears to yield diverse outcomes (acute and chronic inflammation, or cell survival) under distinct conditions [27]. Its elevated expression during IR injury appears to amplify inflammatory and oxidative stress responses such as overproduction of isoprostanes [28]. In this context, 8-isoprostane functions as an oxidative stress marker, initiating a cascade of detrimental processes encompassing lipid peroxidation, protein oxidation, and DNA damage. These events contribute to cellular dysfunction and injury [29]. Moreover, 8-isoprostane is capable of stimulating inflammatory pathways by prompting the release of pro-inflammatory cytokines and chemokines, thereby activating NF- κ B signaling [30]. NF- κ B activation drives the expression of diverse pro-inflammatory genes and adhesion molecules, further augmenting the inflammatory response [25]. Additionally, 8-isoprostane can perturb mitochondrial function, impairing energy production and increasing ROS production. Consequently, this disruption in mitochondrial homeostasis compromises cellular equilibrium and heightens cell susceptibility to apoptosis [30].

MiRs play a crucial role in regulating IR injury by controlling tissue angiogenesis and modifying signaling pathways during ischemia [31,32]. MiR-320 expression significantly increases during IR injury [12]. Inhibiting miR-320 in the current study reduced oxidative stress, inflammation, and brain injury, underscoring its critical role in regulating cerebral IR injury. An interaction between miR-320 and HMGB1, a protein that activates the NF- κ B signaling pathway, has been observed; downregulating HMGB1 has been shown to protect ischemic cells from IR injury [33,34]. We observed a direct relationship between miR-320 and HMGB1. Interestingly, miR-320 overexpression led to elevated HMGB1 expression, while the administration of the HMGB1 antagonist did not influence the upregulation of miR-320 induced by IR but did result in reduced

infarct volumes. It has been shown that in certain tissues, such as hepatocellular carcinoma, miR-320 directly targets HMGB1 [18]. However, the connection between miRs and target protein expression can be intricate and influenced by various regulatory mechanisms. Feedback loops, compensatory mechanisms, and crosstalk with other signaling pathways might explain the contradictory outcomes. Moreover, the response to miR modulation can vary depending on the specific tissue and cellular context. Additionally, miR-320 exhibits distinct expression patterns in different tissues after experiencing ischemic damage, further contributing to diverse outcomes within the complex cascade of cerebral IR conditions.

Inhibition of HMGB1 expression significantly reduced IR injury outcomes and NF- κ B signaling in cerebral tissue, whereas overexpression of miR-320 substantially increased HMGB1 expression. Therefore, miR-320 expression during cerebral IR injury may enhance HMGB1 expression, resulting in increased oxidative stress, inflammatory reactions, and mitochondrial dysfunction. Modulating the miR-320/HMGB1/NF- κ B pathway could regulate the progression of IR injury, and downregulating miR-320 and HMGB1 holds the potential to reduce the occurrence of cerebral IR injury. However, further research is necessary to fully comprehend and confirm the contribution of these findings to IR injury outcomes, particularly in other organs, as well as to explore mitochondrial biogenesis and intra-mitochondrial pathways as critical effector targets of the miR-320/HMGB1/NF- κ B pathway.

Conclusions

In conclusion, the findings of this investigation revealed that downregulating miR-320 had protective benefits against cerebral IR injury in rats by improving mitochondrial function and reducing inflammatory responses and oxidative stress. The modification of components within the HMGB1/NF- κ B pathway by miR-320 was associated with these outcomes, underscoring the therapeutic potential of targeting this pathway for cerebral IR injury.

Conflict of Interest

There is no conflict of interest.

Acknowledgements

This project was funded by a grant from the basic research program (grant No: 2020-KYYWF-0758).

References

1. GBD 2019 Stroke Collaborators. Global, regional, and national burden of stroke and its risk factors, 1990-2019: a systematic analysis for the Global Burden of Disease Study 2019. *Lancet Neurol* 2021;20:795-820. [https://doi.org/10.1016/S1474-4422\(21\)00252-0](https://doi.org/10.1016/S1474-4422(21)00252-0)
2. Lin L, Wang X, Yu Z. Ischemia-reperfusion Injury in the Brain: Mechanisms and Potential Therapeutic Strategies. *Biochem Pharmacol (Los Angel)* 2016;5:213. <https://doi.org/10.4172/2167-0501.1000213>
3. Jurcau A, Simion A. Neuroinflammation in Cerebral Ischemia and Ischemia/Reperfusion Injuries: From Pathophysiology to Therapeutic Strategies. *Int J Mol Sci* 2021;23:14. <https://doi.org/10.3390/ijms23010014>
4. Wu L, Xiong X, Wu X, Ye Y, Jian Z, Zhi Z, Gu L. Targeting Oxidative Stress and Inflammation to Prevent Ischemia-Reperfusion Injury. *Front Mol Neurosci* 2020;13:28. <https://doi.org/10.3389/fnmol.2020.00028>
5. Wong CH, Crack PJ. Modulation of neuro-inflammation and vascular response by oxidative stress following cerebral ischemia-reperfusion injury. *Curr Med Chem* 2008;15:1-14. <https://doi.org/10.2174/092986708783330665>
6. Li S, Wang H, Zhou Y. JAK2/STAT3 pathway mediates beneficial effects of pterostilbene on cardiac contractile and electrical function in the setting of myocardial reperfusion injury. *Physiol Res* 2022;71:489-499. <https://doi.org/10.33549/physiolres.934919>
7. Ye Y, Zeng Z, Jin T, Zhang H, Xiong X, Gu L. The Role of High Mobility Group Box 1 in Ischemic Stroke. *Front Cell Neurosci* 2019;13:127. <https://doi.org/10.3389/fncel.2019.00127>
8. Shi Y, Zhang L, Teng J, Miao W. HMGB1 mediates microglia activation via the TLR4/NF- κ B pathway in coriaria lactone induced epilepsy. *Mol Med Rep* 2018;17:5125-5131. <https://doi.org/10.3892/mmr.2018.8485>
9. Xie W, Zhu T, Dong X, Nan F, Meng X, Zhou P, Sun G, Sun X. HMGB1-triggered inflammation inhibition of notoginseng leaf triterpenes against cerebral ischemia and reperfusion injury via MAPK and NF- κ B signaling pathways. *Biomolecules* 2019;9:512. <https://doi.org/10.3390/biom9100512>
10. Machackova T, Vychytilova-Faltejskova P, Souckova K, Laga R, Androvič L, Mixová G, Slaby O. Barriers in systemic delivery and preclinical testing of synthetic microRNAs in animal models: an experimental study on miR-215-5p mimic. *Physiol Res* 2021;70:481-487. <https://doi.org/10.33549/physiolres.934571>
11. Neag MA, Mitre AO, Burlacu CC, Inceu AI, Mihiu C, Melincovici CS, Bichescu M, Buzoianu AD. miRNA Involvement in Cerebral Ischemia-Reperfusion Injury. *Front Neurosci* 2022;16:901360. <https://doi.org/10.3389/fnins.2022.901360>
12. Zhu XA, Gao LF, Zhang ZG, Xiang DK. Down-regulation of miR-320 exerts protective effects on myocardial I-R injury via facilitating Nrf2 expression. *Eur Rev Med Pharmacol Sci* 2019;23:1730-1741. https://doi.org/10.26355/eurrev_201902_17135
13. Tian ZQ, Jiang H, Lu ZB. MiR-320 regulates cardiomyocyte apoptosis induced by ischemia-reperfusion injury by targeting AKIP1. *Cell Mol Biol Lett* 2018;23:41. <https://doi.org/10.1186/s11658-018-0105-1>
14. Liang L, Wang J, Yuan Y, Zhang Y, Liu H, Wu C, Yan Y. MicRNA-320 facilitates the brain parenchyma injury via regulating IGF-1 during cerebral I/R injury in mice. *Biomed Pharmacother* 2018;102:86-93. <https://doi.org/10.1016/j.biopha.2018.03.036>
15. He F, Shi E, Yan L, Li J, Jiang X. Inhibition of micro-ribonucleic acid-320 attenuates neurologic injuries after spinal cord ischemia. *J Thorac Cardiovasc Surg* 2015;17:398-406. <https://doi.org/10.1016/j.jtcvs.2015.03.066>
16. Ren XP, Wu J, Wang X, Sartor MA, Qian J, Jones K, Qian J, Nicolaou P, Pritchard TJ, Fan GC. MicroRNA-320 Is Involved in the Regulation of Cardiac Ischemia/Reperfusion Injury by Targeting Heat-Shock Protein 20. *Circulation* 2009;119:2357-2366. <https://doi.org/10.1161/CIRCULATIONAHA.108.814145>
17. Tang H, Lee M, Sharpe O, Salamone L, Noonan EJ, Hoang CD, Levine S, ET AL. Oxidative stress-responsive microRNA-320 regulates glycolysis in diverse biological systems. *FASEB J* 2012;26:4710-4721. <https://doi.org/10.1096/fj.11-197467>
18. Yan J, Ying S, Cai X. MicroRNA-Mediated Regulation of HMGB1 in Human Hepatocellular Carcinoma. *Biomed Res Int* 2018;2018:2754941. <https://doi.org/10.1155/2018/2754941>
19. Kim SW, Lee H, Lee HK, Kim ID, Lee JK. Neutrophil extracellular trap induced by HMGB1 exacerbates damages in the ischemic brain. *Acta Neuropathol Commun* 2019;7:94. <https://doi.org/10.1186/s40478-019-0747-x>

20. Banks WA, Hansen KM, Erickson MA, Crews FT. High-mobility group box 1 (HMGB1) crosses the BBB bidirectionally. *Brain Behav Immun* 2023;111:386-394. <https://doi.org/10.1016/j.bbi.2023.04.018>
 21. Stoicea N, Du A, Lakis DC, Tipton C, Arias-Morales CE, Bergese SD. The MiRNA journey from theory to practice as a CNS biomarker. *Front Genet* 2016;7:11. <https://doi.org/10.3389/fgene.2016.00011>
 22. Schaar KL, Brennenman MM, Savitz SI. Functional assessments in the rodent stroke model. *Exp Trans Stroke Med* 2010;2:13. <https://doi.org/10.1186/2040-7378-2-13>
 23. De-Ugarte L, Balcells S, Nogues X, Grinberg D, Diez-Perez A, Garcia-Giralt N. Pro-osteoporotic miR-320a impairs osteoblast function and induces oxidative stress. *PLoS One* 2018;13:e0208131. <https://doi.org/10.1371/journal.pone.0208131>
 24. Wu S, Xu H, Peng J, Wang C, Jin Y, Liu K, Sun H, Qin J. Potent anti-inflammatory effect of dioscin mediated by suppression of TNF- α -induced VCAM-1, ICAM-1 and EL expression via the NF- κ B pathway. *Biochimie* 2015;110:62-72. <https://doi.org/10.1016/j.biochi.2014.12.022>
 25. Jover-Mengual T, Hwang JY, Byun HR, Court-Vazquez BL, Centeno JM, Burguete MC, Zukin RS. The Role of NF- κ B Triggered Inflammation in Cerebral Ischemia. *Front Cell Neurosci* 2021;15:633610. <https://doi.org/10.3389/fncel.2021.633610>
 26. Yang L, Tao LY, Chen XP. Roles of NF-kappaB in central nervous system damage and repair. *Neurosci Bull* 2007;23:307-313. <https://doi.org/10.1007/s12264-007-0046-6>
 27. Sun SC. The non-canonical NF- κ B pathway in immunity and inflammation. *Nat Rev Immunol* 2017;17:545-558. <https://doi.org/10.1038/nri.2017.52>
 28. Liu X, Lin R, Zhao B, Guan R, Li T, Jin R. Correlation between oxidative stress and the NF- κ B signaling pathway in the pulmonary tissues of obese asthmatic mice. *Mol Med Rep* 2016;13:1127-1134. <https://doi.org/10.3892/mmr.2015.4663>
 29. Musiek ES, Yin H, Milne GL, Morrow JD. Recent advances in the biochemistry and clinical relevance of the isoprostane pathway. *Lipids* 2005;40:987-994. <https://doi.org/10.1007/s11745-005-1460-7>
 30. Bauer J, Ripperger A, Frantz S, Ergün S, Schwedhelm E, Benndorf RA. Pathophysiology of isoprostanes in the cardiovascular system: implications of isoprostane-mediated thromboxane A2 receptor activation. *Br J Pharmacol* 2014;171:3115-3131. <https://doi.org/10.1111/bph.12677>
 31. Yin C, Wang X, Kukreja RC. Endogenous microRNAs induced by heat-shock reduce myocardial infarction following ischemia-reperfusion in mice. *FEBS Lett* 2008;582:4137-4142. <https://doi.org/10.1016/j.febslet.2008.11.014>
 32. Jayawardena E, Medzikovic L, Ruffenach G, Eghbali M. Role of miRNA-1 and miRNA-21 in Acute Myocardial Ischemia-Reperfusion Injury and Their Potential as Therapeutic Strategy. *Int J Mol Sci* 2022;23:1512. <https://doi.org/10.3390/ijms23031512>
 33. Nakata K, Okazaki M, Shimizu D, Suzawa K, Shien K, Miyoshi K, Otani S, ET AL. Protective effects of anti-HMGB1 monoclonal antibody on lung ischemia reperfusion injury in mice. *Biochem Biophys Res Commun* 2021;573:164-170. <https://doi.org/10.1016/j.bbrc.2021.08.015>
 34. Mardente S, Mari E, Consorti F, Di Gioia C, Negri R, Etna M, Zicari A, Antonaci A. HMGB1 induces the overexpression of miR-222 and miR-221 and increases growth and motility in papillary thyroid cancer cells. *Oncol Rep* 2012;28:2285-2289. <https://doi.org/10.3892/or.2012.2058>
-